Modeling and Analysis of Skidding and Slipping in Wheeled Mobile Robots: Control Design Perspective

Danwei Wang, *Senior Member, IEEE*, and Chang Boon Low

***Abstract*—This paper aims to give a general and unifying presentation on modeling of wheel mobile robots (WMRs) in the presence of wheel skidding and slipping from the perspective of control design. We present kinematic models that explicitly relate perturbations to the vehicle skidding and slipping. Four configurations of mobile robots are considered, and perturbations due to skidding and slipping are categorically classified as input-additive, input multiplicative, and/or matched/unmatched perturbations. Furthermore, we relate the WMR's maneuverability with the vehicle controllability that provides a measure on the WMR ability to track a trajectory in the presence of wheel skidding and slipping. These classifications and formulations lay a base for the deployments of various control design techniques to overcome the addressed perturbations.**

***Index Terms*—Control perspective, controllability, explicit perturbation descriptions, maneuverability, modeling, tracking, wheel skidding and slipping.**

I. Introduction

WHEELED mobile robots (WMRs) control problems have been intensively studied in recent years; and apparently, most problems have been properly addressed [1]–[16]. However, most existing works assume that WMRs satisfy the nonslipping and nonskidding conditions. In reality, these assumptions cannot be met due to tire deformation and other reasons; hence, stability and control performance of these existing controllers are not guaranteed in real running.

Several controllers have been proposed for the popular Type (2,0) WMR based on a kinematic model constructed in [17] to address the issue of the skidding effect represented by unknown bounded perturbation. Under the assumption of the unknown perturbation being state vanishing, an exponentially stable robust stabilizing controller was proposed for the WMR [17]. Later, the model was used in [18] and [19], and uniform boundedness solutions were proposed for stabilization and tracking problems without assuming the perturbation to be constant or state vanishing. Dixon *et al.* [20] extended their previous paper [8] to address the skidding by designing robust tracking and regulation controllers using the kinematic model. These controllers offer uniform boundedness solutions by robust control approach. However, if a high-precision control performance is desirable, these control laws would require high control input and fast switching actions. These methods can be constrained by implementation and mechanical issues.

In [7], [21], and [22], another framework was proposed to address the WMR tracking control problem in the presence of both skidding and slipping effects. A dynamic model was proposed to analyze the stability of a feedback linearization controller [23] using singular perturbation analysis theory [7]. The analysis shows that the control system remains stable for very mild skidding and slipping. Another linear time-varying controller was proposed [21] to achieve uniformly local exponential stability for the Type (2,0) unicycle based on the dynamic model. In [22], the model is applied to design a slow manifold controller to solve an output-tracking problem. It should be noted that these dynamic models rely on the accurate measurement of the parameter ϵ that is not explicitly expressed in terms of skidding and slipping states; hence, its accurate measurement is difficult to obtain.

Based on the literature [7], [17], we see that the available WMR models do not provide sufficient insights for control design. These perturbations are regarded as unknown terms. In this paper, we derive kinematic models that explicitly relate the perturbations to the vehicle skidding and slipping that are geometrically well defined. This explicit description allows these perturbations to be analyzed from a control perspective. In this paper, four nonholonomic WMR configurations are considered, and perturbations due to skidding and slipping are categorically classified as input-additive, input-multiplicative, and/or matched/unmatched perturbations. A unified framework in terms of the maneuverability index is used to address the controllability of all four WMR configurations. Tracking problem is addressed in this new insight and limitations of control designs/objectives. A preliminary version of the research in this paper was also presented in [24].

Manuscript received February 7, 2007; revised April 12, 2007. This paper was recommended for publication by Associate Editor E. Papadopoulos and Editor F. Park upon evaluation of the reviewers' comments. This paper was presented in part at the Proceedings of the 2006 IEEE/RSJ International Conference on Intelligent Robots and Systems, Beijing, China, and in part at the Proceedings of the 2007 IEEE/International Conference on Robotics and Automation, Rome, April.

D. Wang is with the Division of Control and Instrumentation, School of Electrical and Electronic Engineering, Nanyang Technological University, Singapore 639798, Singapore (e-mail: edwwang@ntu.edu.sg).

C. B. Low is with the DSO National Laboratories, Singapore 118230, Singapore (e-mail: cb@pmail.ntu.edu.sg).

Digital Object Identifier 10.1109/TRO.2008.921563

II. Wheel Modeling Under Skidding and Slipping

This section describes wheel skidding and slipping physically and mathematically. In reality, tire deformation is common, and it is required to translate rotational torques into longitudinal traction force for motion.

A. Skidding

Fig. 1 illustrates a deformed tire in motion. When the wheel negotiates a turn, a lateral force, namely *cornering force*, is

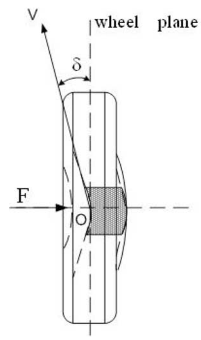

Fig. 1. Tire deformation under a lateral force.

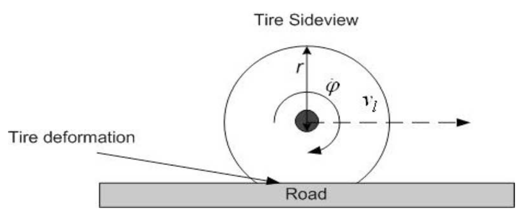

Fig. 2. Tire deformation under weight.

generated by the road–tire interaction [25]. The cornering force acts laterally on the wheel's contact patch, causing the wheel to transverse along a direction away from the wheel's plane. This behavior is referred to as *skidding*. The angle between the wheel's direction of travel and the wheel's plane is known as the *slip angle* δ. When a wheel skids, the nonskidding assumption no longer holds. The lateral force F can be approximately described by $F = C\delta$ for a small slip angle δ.

B. Slipping

Besides wheel skidding, tire deformation causes wheel slippage (Fig. 2). The variable *r* denotes the wheel's free rolling radius with no weight, $\dot{\varphi}$ represents the wheel's angular velocity, and v_l represents the wheel's linear velocity. Under pure rolling assumption where there is no tire deformation, the wheel's linear velocity is $v_l = r\dot{\varphi}$. However, this is not the case for a deformed wheel. The wheel slipping can be characterized by slippage $i = 1 - \frac{v_l}{r\dot{\varphi}}$ that has a value range of $i \in [-1, 1]$. $i = 0$ indicating no wheel slippage whereas $i = 1$ implies a complete slippage, i.e., the wheel is not moving linearly despite its angular rotation. In normal road condition, the wheel's slippage is usually $i \in (-1, 1)$. We also refer the *longitudinal slip velocity* as $d = r\dot{\varphi} - v_l$.

III. Kinematic Model With Skidding and Slipping

In this section, we use the tire deformation described in Section II to develop the kinematic perturbations due to skidding and slipping in term of the slip angle and slip velocity. The notations and definitions used in the following developments are adopted from the well-established work in [2].

We develop kinematic models for four configurations that are generic nonholonomic WMR systems. These four configurations of WMRs are the Type (2,0), (2,1), (1,1), and (1,2). The

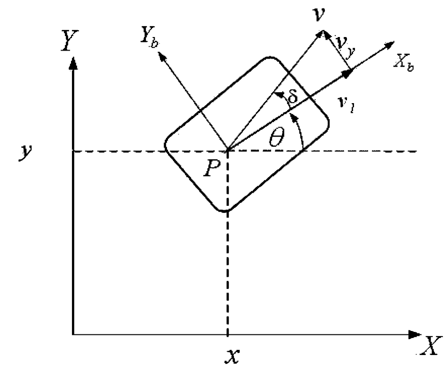

Fig. 3. WMR body frame.

WMRs considered in this paper have a body frame $\{X_b, Y_b\}$ attached to the reference point P with coordinates $\xi = (x, y)^T$ in global coordinate frame $\{X, Y\}$, as shown in Fig. 3. θ denotes the orientation of the basis $\{X_b, Y_b\}$ with respect to the global frame. $\vec{v}$ denotes the velocity of the reference point P, $\vec{v}_y$ represents the velocity $\vec{v}$ projected on the direction of Y_b, and $\vec{v}_l$ denotes the velocity $\vec{v}$ projected on the direction of X_b. These velocities (v_l, v_y) relate to the wheel's slip angle δ by the geometric relationships

$$\tan\delta = \frac{v_y}{v_l}, \qquad \sin\delta = \frac{v_y}{v}. \tag{1}$$

The maneuverability index of a Type (m, s) WMR is defined as the sum of mobility index m and steerability index s [2]. In this paper, all considered WMRs have either maneuverability two (M2) or maneuverability three (M3). In the following development, the control input of a WMR is denoted by $\mathbf{U}$, and the orthogonal rotation matrix is defined as

$$R = \begin{bmatrix} \cos(\theta) & \sin(\theta) \\ -\sin(\theta) & \cos(\theta) \end{bmatrix}. \tag{2}$$

A. Type (2,0) WMR

Fig. 4 depicts a Type (2,0) WMR with M2. This class of WMR can be represented by a simplified model where a fictitious wheel is located at the center of two physical wheels. The reference point P is defined at the center of two physical wheels along the axis between two wheels (see Fig. 4). Fig. 5 depicts the motion of a Type (2,0) WMR with M2 using the simplified model in the presence of skidding and slipping. In the ideal case of pure rolling and nonskidding, the velocity $\vec{v}$ is constrained along X_b. However, when wheel skidding occurs, the velocity $\vec{v}$ deviates from the X_b-axis by an angle δ. $\vec{v}_\perp$ denotes the direction orthogonal to the velocity $\vec{v}$.

To derive the nonholonomic constraint equation in the presence of skidding and slipping, we extend the equation formulation used in the ideal cases [2] to the situations with skidding and slipping. The vector $\vec{v}_\perp$ is orthogonal to $\vec{v}$ and has zero length, i.e.,

$$[-\sin(\delta_2) \quad \cos(\delta_2)]R(\theta)\dot{\xi} = [0] \tag{3}$$

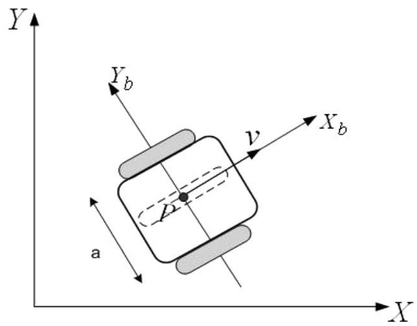

Fig. 4. Type (2,0) WMR: ideal case.

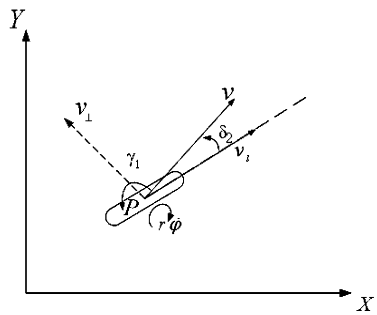

Fig. 5. Type (2,0) WMR: in the presence of skidding and slipping.

which has a solution

$$R(\theta)\dot{\xi} = \alpha_1 \begin{bmatrix} \cos(\delta_2) \\ \sin(\delta_2) \end{bmatrix} \tag{4}$$

with $\alpha_1 \neq 0$ being a scalar. In the global coordinate frame, the solution can be expressed as

$$\dot{\xi} = \alpha_1 \begin{bmatrix} \cos(\theta)\cos(\delta_2) - \sin(\theta)\sin(\delta_2) \\ \sin(\theta)\cos(\delta_2) + \cos(\theta)\sin(\delta_2) \end{bmatrix}.$$

The scalar constant α_1 can be interpreted as the magnitude of WMR's point velocity $\vec{v}$. Using the geometric relation (1), the kinematic model of the WMR can be written as

$$\dot{\xi} = \begin{bmatrix} v_l\cos(\theta) - v_y\sin(\theta) \\ v_l\sin(\theta) + v_y\cos(\theta) \end{bmatrix}. \tag{5}$$

Comparing model (5) with the kinematic model in [17] shows that the general perturbation term $\alpha_1 \sin\delta_2$ can be interpreted as the lateral skidding velocity v_y. The linear velocity of the WMR $v_l$is related to the generalized longitudinal slip velocity d and the velocity control $r\dot{\varphi}$. $r\dot{\varphi}$ denotes the controllable velocity input of the fictitious wheel where $r$and $\dot{\varphi}$ denote the free-rolling radius and angular velocity of the fictitious wheel. In the nonslipping case, it is well known that $r\dot{\varphi} = v_l$. In the case of wheel slipping, the relation between the velocity input and its linear velocity becomes $v_l = r\dot{\varphi} - d$.

The WMR's yaw rate $\dot{\theta}$ can be easily shown as follows:

$$\dot{\theta} = \gamma_1 + \delta_1. \tag{6}$$

γ_1 is the yaw rate input where it is controllable from the angular velocities of the physical wheels and $\delta_1$represents a generalized yaw rate perturbation due to the wheel slippage of the wheels. In the nonslipping case $\delta_1 = 0$, $\dot{\theta} = \gamma_1$. In the case of wheel slipping, there exists an additional yaw rate disturbance that is represented as δ_1 in 6.

Equations (5) and (6) form the following kinematic model:

$$\begin{bmatrix} \dot{x} \\ \dot{y} \\ \dot{\theta} \end{bmatrix} = \begin{bmatrix} v_l\cos(\theta) - v_y\sin(\theta) \\ v_l\sin(\theta) + v_y\cos(\theta) \\ \gamma_1 + \delta_1 \end{bmatrix}. \tag{7}$$

For this Type (2,0) WMR, the control input is $\mathbf{U} = (r\dot{\varphi}, \gamma_1)$. To gain insights into the kinematic perturbations from a control perspective, the perturbations are defined and classified. We rearrange the kinematic model in the following form:

$$\dot{\xi} = (r\dot{\varphi} - \triangle_1)\begin{bmatrix} \cos(\theta) \\ \sin(\theta) \end{bmatrix} + \triangle_2 \tag{8}$$

$$\dot{\theta} = \gamma_1 + \triangle_3 \tag{9}$$

where the perturbations $\{\triangle_1, \triangle_2, \triangle_3\}$ are defined as

$$\triangle_1 = d, \quad \triangle_2 = v_y \begin{bmatrix} -\sin(\theta) \\ \cos(\theta) \end{bmatrix}, \quad \triangle_3 = \delta_1. \tag{10}$$

Property 1: The perturbations $\{\triangle_1, \triangle_2, \triangle_3\}$are classified as: 1) $\triangle_1$ and $\triangle_3$ are input-additive and 2) $\triangle_2$ is unmatched.

These classifications can be easily identified from (8) and (9). The perturbations $\triangle_1$ and $\triangle_3$ are input-additive by inspection. On the other hand, the perturbation vector $\triangle_2$ is always orthogonal to input vector $(\cos(\theta), \sin(\theta))^T$, and thus is unmatched.

Property 2: Suppose that $\{\delta_1, \delta_2, d, v_l\}$ are bounded with $|\delta_1| < \rho_1$, $|\delta_2| < \rho_2 < \frac{\pi}{2}$, $|d| < \rho_3$, $|v_l| < \rho_4$ where ρ_i, $i = 1, 2, 3, 4$, are positive constants. The perturbations $\{\triangle_1$, $\triangle_2$, and $\triangle_3\}$ are bounded as follows:

$$|\triangle_1| < \rho_3, \quad ||\triangle_2|| < \rho_4 \tan\rho_2, \quad |\triangle_3| < \rho_1 \tag{11}$$

Proof: Inequalities $|\triangle_1| < \rho_3$, $|\triangle_3| < \rho_1$ are implied from (10) with assumptions $|d| < \rho_3$ and $|\delta_1| < \rho_1$. The geometric relation (1) leads to $v_y = v_l \tan\delta_2$; and hence, $|v_y| < \rho_4 \tan(\rho_2)$. This implies that $||\triangle_2|| = |v_y|\,||[\cos\theta \sin\theta]^T|| \leq \rho_4 \tan(\rho_2)$ because of $||[\cos\theta \;\; \sin\theta]^T|| = 1$.

Remark 1: The kinematic perturbations of this configuration are classified as *input-additive* and *unmatched*. The types of perturbations suggest the difficulty levels in compensating these perturbations from a control perspective. For instance, input-additive perturbation is located in the same channel with a control input and can be eliminated without much difficulty if the instantaneous perturbation is known or measurable. On the other hand, *unmatched perturbation* does not fall into any channel with a control input. This unique characteristic suggests that any undesirable effects due to this unmatched perturbation cannot be compensated directly (without using other dynamical states) or in some cases cannot be compensated at all.

B. Type (1,1) WMR

The configuration of Type (1,1) car-like WMR is shown in Fig. 6. The WMR is equipped with a front-centered steerable wheel and fixed parallel rear wheels. Similarly, the fixed parallel wheels can be simplified by a fictitious wheel at the center of the fixed parallel wheels. As shown in Fig. 6, the reference point P of this WMR is defined on the center of the two rear wheels'

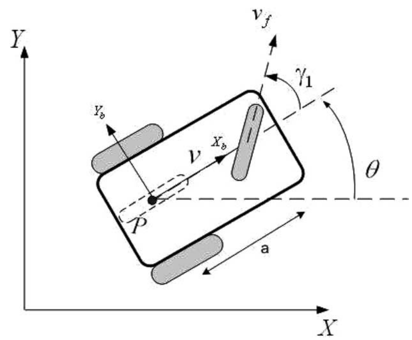

Fig. 6. Type (1,1) WMR: ideal case.

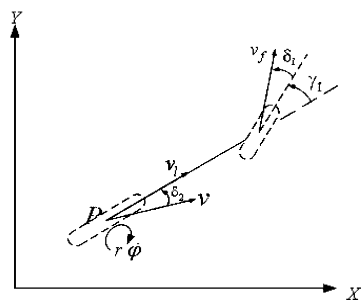

Fig. 7. Type (1,1) WMR: in the presence of skidding and slipping.

rolling axis. Fig. 7 shows the motion of the WMR using the simplified model. γ_1 denotes the WMR's front steering angle, a denotes the WMR's wheelbase, δ_1 represents the slip angle of the front wheel, and δ_2 represents the generalized slip angle of the rear fictitious wheel. This type of WMR has maneuverability index 2 (M2).

The rear fixed wheel leads to the following constraint equation by projecting velocity $\vec{v}$ along $\vec{v}_\perp$:

$$[-\sin(\delta_2) \quad \cos(\delta_2)]\, R(\theta)\dot{\xi} = [0]. \tag{12}$$

For the front steerable wheel, we obtain

$$[-\sin(\delta_1+\gamma_1) \quad \cos(\delta_1+\gamma_1)]\, R(\theta)\dot{\xi} + a\cos(\delta_1+\gamma_1)\dot{\theta} = [0]. \tag{13}$$

A solution to (12) and (13) is

$$\begin{bmatrix} R(\theta)\dot{\xi} \\ \dot{\theta} \end{bmatrix} = \alpha_1 \begin{bmatrix} \cos(\delta_2) \\ \sin(\delta_2) \\ \dfrac{\sin(\delta_1+\gamma_1)\cos(\delta_2) - \cos(\delta_1+\gamma_1)\sin(\delta_2)}{a\cos(\delta_1+\gamma_1)} \end{bmatrix}. \tag{14}$$

The scalar α_1 can be interpreted as the velocity magnitude v. Expressing the solution (14) in the global coordinate frame leads to the kinematic model

$$\begin{bmatrix} \dot{x} \\ \dot{y} \\ \dot{\theta} \end{bmatrix} = \begin{bmatrix} v_l\cos(\theta) - v_y\sin(\theta) \\ v_l\sin(\theta) + v_y\cos(\theta) \\ \frac{v_l}{a}\tan(\gamma_1+\delta_1) - \frac{v_y}{a} \end{bmatrix}. \tag{15}$$

This WMR has a linear velocity $v_l = r\dot{\varphi} - d$ and control input $\mathbf{U} = (r\dot{\varphi},\ \gamma_1)$. Similarly, $r\dot{\varphi}$ represents the velocity control of the fictitious wheel, where d is the generalized slip velocity of the rear wheels.

To model the perturbations due to wheel skidding and slipping, the kinematic model (15) can be expressed as follows, using (14):

$$\dot{\xi} = (r\dot{\varphi} - \triangle_1)\begin{bmatrix} \cos(\theta) \\ \sin(\theta) \end{bmatrix} + \triangle_2 \tag{16}$$

$$\dot{\theta} = (r\dot{\varphi} - \triangle_1)\frac{1}{a}\tan(\gamma_1 + \triangle_3) + \triangle_4 \tag{17}$$

where the perturbations $\{\triangle_1, \triangle_2, \triangle_3, \triangle_4\}$ are

$$\triangle_1 = d, \quad \triangle_2 = v_y\begin{bmatrix} -\sin(\theta) \\ \cos(\theta) \end{bmatrix}, \quad \triangle_3 = \delta_1, \quad \triangle_4 = -\frac{v_y}{a}. \tag{18}$$

Property 3: The perturbations $\{\triangle_1, \triangle_2, \triangle_3, \triangle_4\}$ are classified as follows: 1) $\triangle_1$ and $\triangle_3$ are input-additive; 2) $\triangle_2$ is unmatched; and 3) $\triangle_4$ is matched.

By inspection, it is clear that $\triangle_1, \triangle_3$ are input-additive and $\triangle_4$ is matched. Similarly, by following the same arguments used in Type (2,0) case, we can show $\triangle_2$ being unmatched.

Property 4: Suppose that $\{\delta_1, \delta_2, d, v_l\}$ satisfy $|\delta_1| < \rho_1 < \frac{\pi}{2}$, $|\delta_2| < \rho_2 < \frac{\pi}{2}$, $|d| < \rho_3$, and $|v_l| < \rho_4$ where ρ_i, $i = 1, 2, 3, 4$ are positive constants. Then, the perturbations $\{\triangle_1, \triangle_2, \triangle_3, \triangle_4\}$ satisfy

$$|\triangle_1| < \rho_3, |\triangle_2| < \rho_4\tan\delta_2 \tag{19}$$

$$|\triangle_3| < \rho_1, |\triangle_4| < \frac{1}{a}\rho_4\tan\rho_2. \tag{20}$$

By following the same arguments used in the case of Type (2,0), we can show that the perturbations $\{\triangle_1, \triangle_2, \triangle_3, \triangle_4\}$satisfy the bounds since the wheelbase a of the WMR is a positive finite constant.

Remark 2: Contrast to unmatched perturbation, a matched perturbation is located in a channel with a control input. However, when compared with input-additive perturbation, matched perturbation requires more information for compensation. For instance, suppose that the matched perturbation $\triangle_4$ is known or measurable, we still require reliable information on $(r\dot{\varphi}, \gamma_1, \triangle_1, \triangle_3)$ to compensate the undesirable effects from $\triangle_4$ using computed torque control technique. Nevertheless, this type of perturbation can still be compensated instantaneously from a control input.

C. Type (2,1) WMR

The configuration of a Type (2,1) WMR is shown in Fig. 8. The WMR has a centered steerable wheel and off-centered steerable wheels. Likewise, the off-centered steerable wheels can be represented by one simplified fictitious off-centered steerable wheel between two physical off-centered wheels. The reference P is located on the center of the centered steerable wheel. Fig. 9 shows the motion of the WMR in the presence of wheel skidding and slipping using the simplified model. This class of WMR is equipped with two directional control inputs. γ_2 denotes the front steering angle, α is the angle of the off-centered wheel, δ_2 represents the front slip angle, δ_1 represents the slip angle of the

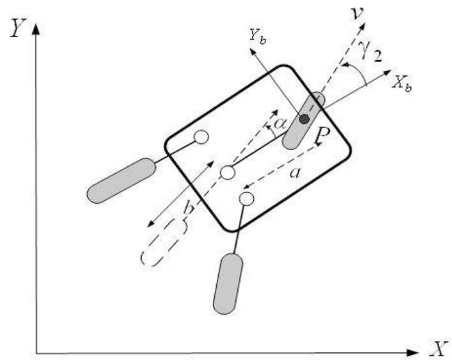

Fig. 8. Type (2,1) WMR: ideal case.

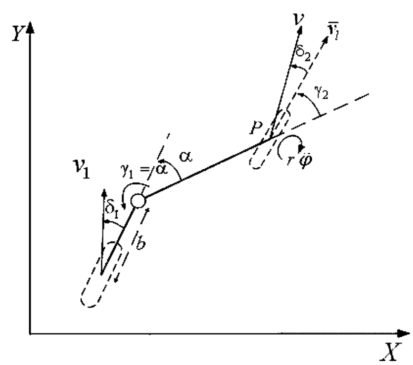

Fig. 9. Type (2,1) WMR: in the presence of skidding and slipping.

fictitious off-centered wheel, and (b, a) represent the respective lengths from the pivots to the wheels, respectively. This WMR has maneuverability index 3 (M3).

The centered steerable wheel leads to the following equation by projecting the velocity $\vec{v}$ along $\vec{v}_\perp$:

$$[-\sin(\gamma_2+\delta_2) \quad \cos(\gamma_2+\delta_2)]\, R(\theta)\dot{\xi} = [0]. \tag{21}$$

A solution for the constraint equation (21) is

$$R(\theta)\dot{\xi} = \alpha_1 \begin{bmatrix} \cos(\gamma_2+\delta_2) \\ \sin(\gamma_2+\delta_2) \end{bmatrix}. \tag{22}$$

We choose $\alpha_1 = v$ and the solution in global coordinates is

$$\begin{bmatrix} \dot{x} \\ \dot{y} \end{bmatrix} = v \begin{bmatrix} \cos(\theta+\gamma_2+\delta_2) \\ \sin(\theta+\gamma_2+\delta_2) \end{bmatrix}. \tag{23}$$

The WMR's yaw rate can be derived by projecting the velocity vector $\vec{v}_1$ of the off-centered wheels along $\vec{v}_{1\perp}$, i.e.,

$$\begin{aligned} &[-\sin(\gamma_2+\delta_2)\cos(\gamma_2+\delta_2)]\, R(\theta)\dot{\xi} - a\dot{\theta}\cos(\alpha+\delta_1) \\ &\quad - (\gamma_1+\dot{\theta})b\cos(\delta_1) = [0]. \end{aligned} \tag{24}$$

Substituting (22) into (24) yields

$$\begin{aligned} &v\sin(\gamma_2+\delta_2)\cos(\alpha+\delta_1) - v\cos(\gamma_2+\delta_2)\sin(\alpha+\delta_1) \\ &\quad - a\dot{\theta}\cos(\alpha+\delta_1) - (\gamma_1+\dot{\theta})b\cos(\delta_1) = 0. \end{aligned} \tag{25}$$

Solving (25) leads to

$$\dot{\theta} = \frac{v\sin(\gamma_2+\delta_2-\alpha-\delta_1) - \gamma_1 b\cos(\delta_1)}{a\cos(\alpha+\delta_1)+b\cos(\delta_1)}. \tag{26}$$

Equations (23) and (26) form the kinematic model of this WMR. The WMR's front steerable wheel has a linear velocity $\bar{v}_l = r\dot{\varphi} - d$. In the same way as the preceding configurations, $r\dot{\varphi}$ represents the velocity control of the wheel, where d is the wheel's slip velocity. Hence, the control inputs for this WMR is $\mathbf{U} = (r\dot{\varphi},\ \gamma_1,\ \gamma_2)$. To model the perturbations due to wheel skidding and slipping, we express the kinematic model as

$$\dot{\xi} = \{r\dot{\varphi}\triangle_1 - \triangle_2\} \begin{bmatrix} \cos(\theta+\gamma_2+\triangle_3) \\ \sin(\theta+\gamma_2+\triangle_3) \end{bmatrix} \tag{27}$$

$$\dot{\theta} = \triangle_4 + \triangle_5\gamma_1 \tag{28}$$

where the perturbations $\{\triangle_1, \triangle_2, \triangle_3, \triangle_4, \triangle_5\}$are defined as

$$\begin{aligned} &\triangle_1 = \frac{1}{\cos\delta_2}, \qquad \triangle_2 = \frac{d}{\cos\delta_2} \qquad \triangle_3 = \delta_2, \\ &\triangle_4 = \frac{v\sin(\gamma_2+\delta_2-\alpha-\delta_1)}{a\cos(\alpha+\delta_1)+b\cos(\delta_1)} \\ &\triangle_5 = \frac{b\cos\delta_1}{a\cos(\alpha+\delta_1)+b\cos(\delta_1)}. \end{aligned}$$

Property 5: The perturbations $\{\triangle_1, \triangle_2, \triangle_3, \triangle_4, \triangle_5\}$are classified as follows: 1) $\triangle_2$ and $\triangle_3$are input-additive; 2) $\triangle_1$ and $\triangle_5$ are input multiplicative; and 3) $\triangle_4$ is matched.

Property 6: Suppose $|\alpha+\delta_1| < \frac{\pi}{2}$, $|\delta_1| < \rho_1 < \frac{\pi}{2}$, $|\delta_2| < \rho_2 < \frac{\pi}{2}$, $|d| < \rho_3$, $|v_l| < \rho_4$, $|\alpha| < \rho_5$ where ρ_i, $i = 1, 2, 3, 4, 5$, are positive constants, then the perturbations $\{\triangle_1, \triangle_2, \triangle_3, \triangle_4, \triangle_5\}$ satisfy

$$\begin{aligned} &1 \le |\triangle_1| < \frac{1}{\cos\rho_2}, \qquad |\triangle_2| \le \frac{\rho_3}{\cos\rho_2}, \qquad |\triangle_3| < \rho_2 \\ &|\triangle_4| < \frac{\rho_4}{\cos\rho_2}\left(\frac{1}{a\cos(\rho_1+\rho_5)+b\cos\rho_1}\right) \\ &0 < \frac{b\cos\rho_1}{a+b} \le |\triangle_5| < \frac{b}{a\cos(\rho_1+\rho_5)+b\cos\rho_1}. \end{aligned}$$

Proof: By definition, $\triangle_1 = \frac{1}{\cos\delta_2}$. It is clear that $\triangle_1$ is lower bounded by unity and upper bounded by $\frac{1}{\cos\rho_2}$. Similarly, the upper and lower bounds of perturbation $\triangle_2$ can be determined since d satisfies $|d| \le \rho_3$. As for perturbation $\triangle_3$, its bound can be established by assumption $|\delta_2| < \rho_2$.

Next, before we show the bounds of perturbations $\triangle_4, \triangle_5$, we claim that $a\cos(\alpha+\delta_1)+b\cos\delta_1$ and $|v|$ satisfy

$$a\cos(\rho_1+\rho_5)+b\cos\rho_1 \le a\cos(\alpha+\delta_1)+b\cos\delta_1 \le a+b \tag{29}$$

and

$$|v| \le \frac{\rho_4}{\cos\rho_2}. \tag{30}$$

Inequality (29) can be shown since $a\cos(\alpha+\delta_1)$ and $b\cos\delta_1$ satisfy, respectively,

$$a\cos(\rho_1+\rho_5) \le a\cos(\alpha+\delta_1) \le a \tag{31}$$

$$b\cos(\rho_1) \le b\cos(\delta_1) \le b. \tag{32}$$

Inequality (30) can be easily obtained by geometric relation $v\cos\delta_2 = v_l$.

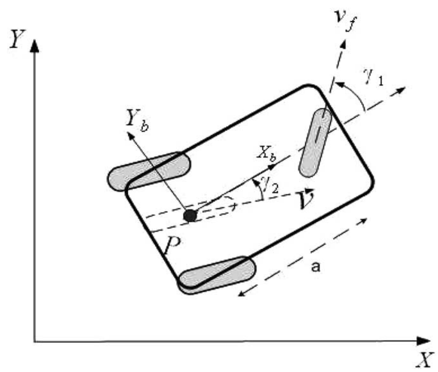

Fig. 10. Type (1,2) WMR: ideal case.

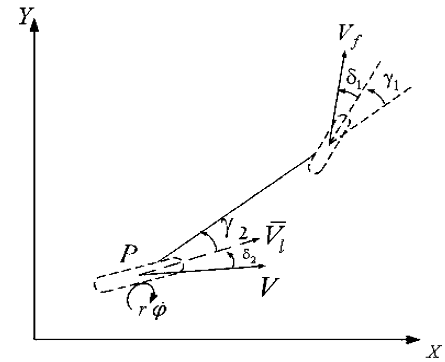

Fig. 11. Type (1,2) WMR: in the presence of skidding and slipping.

From inequality (29), we have

$$\frac{1}{a+b}\leq\frac{1}{a\cos(\alpha+\delta_1)+b\cos\delta_1}\leq\frac{1}{a\cos(\rho_1+\rho_5)+b\cos\rho_1}. \tag{33}$$

Furthermore, we have

$$|v\sin(\gamma_2+\delta_2-\alpha-\delta_1)|\leq|v|\leq\frac{\rho_4}{\cos\rho_2}. \tag{34}$$

Inequalities (33) and (34) lead to

$$|\triangle_4|<\frac{\rho_4}{\cos\rho_2}\left(\frac{1}{a\cos(\rho_1+\rho_5)+b\cos\rho_1}\right). \tag{35}$$

Finally, the bounds of $|\triangle_5|$ can be established using inequalities (32) and (33).

Remark 3: Input multiplicative perturbation distorts the control input that commands the system state. This perturbation can completely disable the control input if the perturbation tends to zero. Fortunately, we have shown that the multiplicative perturbation $\triangle_5$ is lower bounded above zero for this type of WMR. Hence, perturbation $\triangle_5$ will not disable control input γ_1.

D. Type (1,2) WMR

The configuration of the Type (1,2) WMR is shown in Fig. 10. This class of WMR is identified by the centered front and rear steerable wheels. Similarly, rear-centered steerable wheels can be simplified by a fictitious centered steerable wheel at the center of the two physical wheels. The reference point P is defined at the center of two rear steerable wheels (see Fig. 10). This WMR has maneuverability 3 (M3). Fig. 11 depicts the motion of the WMR in the presence of wheel skidding and slipping using the simplified model. γ_1 represents the front steering angle and γ_2 denotes the steering angle of the rear fictitious wheel. a denotes the WMR's wheelbase and $\vec{v}$ the WMR's velocity, δ_1 denotes the slip angle of the front wheel, and δ_2 represents the generalized slip angle of the rear fictitious wheel.

By projecting velocity $\vec{v}$ along $\vec{v}_\perp$, we obtain

$$[\,-\sin(\delta_2+\gamma_2)\quad\cos(\delta_2+\gamma_2)\,]\,R(\theta)\dot{\xi}=[0]. \tag{36}$$

As for the front steerable wheel, we have

$$\begin{aligned}&[\,-\sin(\delta_1+\gamma_1)\cos(\delta_1+\gamma_1)\,]\,R(\theta)\dot{\xi}\\&\quad+a\cos(\delta_1+\gamma_1)\dot{\theta}=[0].\end{aligned} \tag{37}$$

A solution for (36) and (37) is

$$\begin{bmatrix}R(\theta)\dot{\xi}\\ \dot{\theta}\end{bmatrix}=\alpha_1\times\begin{bmatrix}\cos(\gamma_2+\delta_2)\\ \sin(\gamma_2+\delta_2)\\ \dfrac{\sin(\delta_1+\gamma_1)\cos(\gamma_2+\delta_2)-\cos(\delta_1+\gamma_1)\sin(\gamma_2+\delta_2)}{a\cos(\delta_1+\gamma_1)}\end{bmatrix} \tag{38}$$

where α_1 can be interpreted as velocity magnitude v. Similarly, the kinematic model with slipping and skidding can be written as

$$\begin{bmatrix}\dot{x}\\ \dot{y}\\ \dot{\theta}\end{bmatrix}=\begin{bmatrix}v\cos(\theta+\gamma_2+\delta_2)\\ v\sin(\theta+\gamma_2+\delta_2)\\ \dfrac{v\tan(\gamma_1+\delta_1)\cos(\gamma_2+\delta_2)}{a}-\dfrac{v\sin(\gamma_2+\delta_2)}{a}\end{bmatrix}. \tag{39}$$

The longitudinal velocity of the rear steerable wheel is denoted by $\bar{v}_l$ and has the relationship with the wheel's slip velocity and control input $r\dot{\varphi}$ via $\bar{v}_l=r\dot{\varphi}-d$. Similarly, $r\dot{\varphi}$ is the velocity control of the fictitious wheel, where d is the generalized slip velocity of the wheel. The control input of this WMR can be denoted as $\mathbf{U}=(r\dot{\varphi},\gamma_1,\gamma_2)$. The kinematic model can be expressed as

$$\dot{\xi}=(r\dot{\varphi}\triangle_1-\triangle_2)\begin{bmatrix}\cos(\theta+\gamma_2+\triangle_3)\\ \sin(\theta+\gamma_2+\triangle_3)\end{bmatrix} \tag{40}$$

$$\begin{aligned}\dot{\theta}&=(r\dot{\varphi}\triangle_1-\triangle_2)\frac{1}{a}\tan(\gamma_1+\triangle_4)\cos(\gamma_2+\triangle_3)\\&\quad+\frac{(r\dot{\varphi}\triangle_1-\triangle_2)\sin(\gamma_2+\triangle_3)}{a}\end{aligned} \tag{41}$$

where the perturbations $\{\triangle_1,\triangle_2,\triangle_3,\triangle_4\}$ are

$$\triangle_1=\frac{1}{\cos\delta_2},\qquad\triangle_2=\frac{d}{\cos\delta_2},\qquad\triangle_3=\delta_2,\qquad\triangle_4=\delta_1. \tag{42}$$

Property 7: The perturbations $\{\triangle_1,\triangle_2,\triangle_3,\triangle_4\}$ are classified as follows: 1) $\triangle_2$, $\triangle_3$, and $\triangle_4$ are input-additive and 2) $\triangle_1$ is input multiplicative.

This statement can be easily seen from (40) and (41).

Property 8: Suppose that $|\delta_1| < \rho_1 < \frac{\pi}{2}$, $|\delta_2| < \rho_2 < \frac{\pi}{2}$, $|d| < \rho_3$ and $|v_l| < \rho_4$, where $\rho_i, i = 1, 2, 3, 4$ are positive constants. The perturbations $\{\triangle_1, \triangle_2, \triangle_3, \triangle_4\}$ satisfy

$$1 \leq |\triangle_1| \leq \frac{1}{\cos\rho_2}, \qquad |\triangle_2| \leq \frac{\rho_3}{\cos\rho_2} \tag{43}$$

$$|\triangle_3| \leq \rho_2, \qquad |\triangle_4| \leq \rho_1. \tag{44}$$

Property 8 can be shown similarly to Type (2,1) WMR. The lower bound of the multiplicative perturbation $|\triangle_1| \geq 1$ implies that the velocity control input $r\dot{\varphi}$ will not be disabled by $\triangle_1$. Other perturbations $\{\triangle_2, \triangle_3, \triangle_4\}$ influence the WMR's control in a similar fashion as in the preceding configurations.

Remark 4: In this kinematic modeling, the wheel skidding and slipping behaviors are characterized by the generalized perturbations (δ_1, δ_2, d). In the remaining of the paper, these generalized descriptions are utilized to gain useful insights on the mobile robot control problems in the presence of wheel skidding and slipping.

IV. Controllability

This section addresses the controllability of WMRs in the presence of wheel skidding and slipping. Without loss of generality, the kinematic models of the WMRs can be written in the form of

$$\dot{\xi} = f^1_{m+s}(\theta, \mathbf{U}, \delta_2, d) \tag{45}$$

$$\dot{\theta} = f^2_{m,s}(\theta, \mathbf{U}, \delta_1, \delta_2, d) \tag{46}$$

where $\mathbf{U}$ denotes the control inputs of the WMR and vector $f^1_{m+s} \in R^2$ and $f^2_{m,s} \in R$ are given as follows depending on the WMR's maneuverability index.

For WMRs with M2, the vectors f^1 and f^2 are

$$f^1_2 = \begin{bmatrix} v_l\cos(\theta) - v_y\sin(\theta) \\ v_l\sin(\theta) + v_y\cos(\theta) \end{bmatrix} \tag{47}$$

$$f^2_{2,0} = \gamma_1 + \delta_1 \tag{48}$$

$$f^2_{1,1} = \frac{v_l\tan(\gamma_1 + \delta_1)}{a} - \frac{v_y}{a} \tag{49}$$

with the WMR linear velocity $v_l = r\dot{\varphi} - d$ as modeled in Section II and the control inputs $\mathbf{U} = (r\dot{\varphi}, \gamma_1)$. For WMRs with maneuverability three (M3), the vectors $f^1_3, f^2_{2,1}, f^2_{1,2}$ are

$$f^1_3 = \begin{bmatrix} v\cos(\theta + \gamma_2 + \delta_2) \\ v\sin(\theta + \gamma_2 + \delta_2) \end{bmatrix} \tag{50}$$

$$f^2_{2,1} = \frac{v\sin(\gamma_2 + \delta_2 - \alpha - \delta_1) - \gamma_1 b\cos(\delta_1)}{a\cos(\alpha + \delta_1) + b\cos(\delta_1)} \tag{51}$$

$$f^2_{1,2} = \frac{v\tan(\gamma_1 + \delta_1)\cos(\gamma_2 + \delta_2)}{a} - \frac{v\sin(\gamma_2 + \delta_2)}{a}. \tag{52}$$

The longitudinal wheel velocity $\bar{v}_l$, as shown in Figs. (9) and (11), is related with the wheel's slip velocity and velocity control $r\dot{\varphi}$ via $\bar{v}_l = r\dot{\varphi} - d$. The control input of this WMR with M3 is $\mathbf{U} = (r\dot{\varphi}, \gamma_1, \gamma_2)$.

Assumption 1: Perturbations $\{\delta_1, \delta_2, d, \dot{\delta}_2, v_y, \dot{v}_y\}$ are bounded and measurable with $|\delta_2| < \frac{\pi}{2}$.

Assumption 1 implies the perturbations are bounded and measurable. Positive theoretical and experimental works have been developed in measuring these perturbations for control using RTK-GPS and other aiding sensors [26]–[28].

In the ideal case where *nonslipping* and *nonskidding* assumptions are satisfied, the controllability of a WMR is referred to as the ability to steer it from an initial posture to a final posture in a finite time, as stated as follows [29].

Definition 1: A WMR is said to be posture controllable if there exists a piecewise continuous input to steer the WMR's configuration (x, y, θ) from an initial posture $\{x(t_0),\ y(t_0),\ \theta(t_0)\}$ to a final posture $\{x(t_f),\ y(t_f),\ \theta(t_f)\}$ in a finite-time interval.

In the presence of wheel skidding, WMRs with M2 do not have posture controllability. Nevertheless, these WMRs should be able to achieve point control by performing appropriate steering action to compensate the skidding and slipping.

Definition 2: A WMR is said to be point controllable if there exists a piecewise continuous input to steer the WMR's reference point P from an initial point $\{x(t_0),\ y(t_0)\}$ to a final point $\{x(t_f),\ y(t_f)\}$ in a finite-time interval.

Now, we show that the kinematic model of a WMR with M2 can be transformed into a form similar to the ideal kinematic model of a Type (2,0) [30] without wheel skidding and slipping.

Lemma 1: Consider a WMR with M2. Suppose that the perturbations $\{\delta_1, \delta_2, d\}$ satisfy Assumption 1. Then, there exists an invertible coordinate transformation and a corresponding invertible input change, respectively

$$\bar{q} = \phi(q, \delta_2), \tag{53}$$

$$\mu = \beta_1(q, \delta_1, \delta_2, d, \mathbf{U}) \tag{54}$$

such that the transformed system becomes

$$\dot{\bar{q}} = G(\bar{q})\mu \tag{55}$$

where

$$\bar{q} = \begin{bmatrix} x \\ y \\ \bar{\theta} \end{bmatrix}, \qquad G(\bar{q}) = \begin{bmatrix} \cos\bar{\theta} & 0 \\ \sin\bar{\theta} & 0 \\ 0 & 1 \end{bmatrix}, \qquad \mu = \begin{bmatrix} v \\ \omega \end{bmatrix} \tag{56}$$

with $\bar{\theta} = \theta + \delta_2$.

Proof: The proof is straightforward and constructive. Define $\bar{q}$ and μ as

$$\bar{q} = [xy\theta + \delta_2]^T \tag{57}$$

$$\mu = \begin{bmatrix} \frac{r\dot{\varphi} - d}{\cos\delta_2} & f^2_{m,s} \end{bmatrix}^T. \tag{58}$$

By inspection, the transformation equation (57) is invertible. We show that the input change (54) is also invertible. It is clear from (58) that the auxiliary v is invertible with respect to $r\dot{\varphi}$. As for ω, we need to show that $\omega = f^2_{m,s}$ is invertible for $\forall(m, s) \in \{(2,0), (1,1)\}$. For the Type (2,0) case, $\omega = \gamma_1 + \delta_1$; hence, it is invertible with respect to γ_1 since it is linear. As for Type (1,1), ω is defined as

$$\omega = \frac{v\tan(\gamma_1 + \delta_1)\cos(\delta_2)}{a} - \frac{v\sin(\delta_2)}{a}. \tag{59}$$

With some manipulations, we have

$$\gamma_1 = \tan^{-1}\left\{\frac{\omega a}{v\cos\delta_2} + \tan\delta_2\right\} - \delta_1. \tag{60}$$

For any nonzero v, ω is invertible; hence, the kinematic model of a WMR with M2 can be converted into (55). With Lemma 1, we can state the following result.

Theorem 1: Suppose that the perturbations $\{\delta_1, \delta_2, d\}$ of a WMR with M2 satisfy Assumption 1, then the WMR is point controllable, but not posture controllable.

Proof: By Lemma 1, the kinematic model of a WMR with M2 can be transformed into (55), where input vector fields are

$$g_1 = \begin{bmatrix}\cos\bar{\theta}\\ \sin\bar{\theta}\\ 0\end{bmatrix},\ g_2 = \begin{bmatrix}0\\0\\1\end{bmatrix}. \tag{61}$$

Let $\triangle$ be the distribution generated by the vector fields $\{g_1, g_2\}$. By applying the controllability result, as in the Appendix, we have

$$\begin{aligned} rank\{\triangle_C\} &= rank\{\mathrm{span}(g_1, g_2, [g_1, g_2])\}\\ &= 3 \end{aligned} \tag{62}$$

for all $\bar{\theta}$. The fact $rank\{\triangle_C\} = 3$ indicates that the system is controllable in coordinates $\bar{q}$. Since ξ is a subvector of $\bar{q}$, controllability in $\bar{q}$ implies controllability in $[x,\ y]^T$ coordinates.

To show that a WMR with M2 is not *posture controllable* in the presence of skidding and slipping, we consider the point subsystem of a WMR with M2,

$$\begin{bmatrix}\dot{x}\\ \dot{y}\end{bmatrix} = v\begin{bmatrix}\cos(\bar{u})\\ \sin(\bar{u})\end{bmatrix} \tag{63}$$

where we define $\bar{u} = \theta + \delta_2$. If the reference point of the WMR ξ is to be steered from an initial point $\xi(0)$ to a final point $\xi(t_f)$, then the directional input control $\bar{u}$ will be constrained along a feasible $\bar{u}_s(t)$ to achieve this goal. This implies that the orientation of the WMR must satisfy $\theta(t) = \bar{u}_s(t) - \delta_s(t)$ to reach the desired point ξ_f. Since, in general, the desired orientation $\theta_d(t)$ of a path that the WMR follows is not $\bar{u}_s(t) - \delta_s(t)$, we conclude that the orientation of the WMR with M2 cannot be equal to $\theta_d(t)$ in order to maintain point controllability. Hence, it is not posture controllable.

Remark 5: Contrast to WMRs with M2, the additional orientation input γ_2 of a WMR with M3 suggests that this class of WMRs can handle the skidding perturbation more effectively. To confirm this intuition, we examine the controllability of the WMRs with M3.

Lemma 2: Consider a WMR with M3. Suppose that the perturbations $\{\delta_1, \delta_2, d\}$ satisfy Assumption 1, then there exists an invertible input change,

$$\mu = \beta_2(q, \delta_1, \delta_2, d, \mathbf{U}) \tag{64}$$

such that the kinematic model of a WMR with M3 becomes

$$\dot{q} = G(q)\mu \tag{65}$$

where

$$\dot{q} = \begin{bmatrix}\dot{\xi}\\ \dot{\theta}\end{bmatrix},\ G(q) = \begin{bmatrix}\cos\theta & 0\\ \sin\theta & 0\\ 0 & 1\end{bmatrix},\ \mu = \begin{bmatrix}v\\ \omega\end{bmatrix}. \tag{66}$$

Proof: By choosing $\gamma_2 = -\delta_2$ and auxiliary input

$$v = \frac{r\dot{\varphi} - d}{\cos\delta_2} \tag{67}$$

the point subsystem of a WMR with M3 becomes

$$\dot{x} = v\cos(\theta) \tag{68}$$

$$\dot{y} = v\sin(\theta). \tag{69}$$

Similarly, the auxiliary input (67) is invertible. Consider the orientation subsystem for a WMR with M3. For Type (1,2) WMR, the auxiliary inputs are defined as

$$\omega = \frac{v}{a}\tan(\gamma_1 + \delta_1). \tag{70}$$

It is clear that auxiliary input (70) is invertible

$$\gamma_1 = \tan^{-1}\left(\frac{\omega a}{v}\right) - \delta_1 \tag{71}$$

for $v \neq 0$.

As for Type (2,1) WMR, we define the auxiliary input for the WMR's orientation subsystem as

$$\omega = \frac{-v\sin(\alpha + \delta_1) - \gamma_1 b\cos(\delta_1)}{a\cos(\alpha + \delta_1) + b\cos(\delta_1)}. \tag{72}$$

We can see that the auxiliary input (72) is invertible under the condition $|a\cos(\alpha + \delta_1) + b\cos(\delta_1)| > 0$ that can be easily met in practice.

Lemmas 1 and 2 imply the matched perturbations can be decoupled by direct compensation if the skidding and slipping parameters are measurable. Lemma 2 leads the following result.

Theorem 2: Suppose that the perturbations $\{\delta_1, \delta_2, d\}$of a WMR with M3 satisfy Assumption 1, then the WMR is *posture controllable*.

Proof: By Lemma 2, the kinematic model of a WMR with M3 is input-equivalent to a nominal Type (2,0) kinematic model (66) that has an rank 3 accessibility distribution

$$\dim\triangle_c = 3. \tag{73}$$

Hence, the WMR is posture controllable.

Remark 6: Theorem 2 suggests that in the presence of skidding and slipping, a WMR with M3 is more controllable when compared with a WMR with M2. Despite the high capability exhibited by the WMRs with M3, these WMRs can inherit a structural property of a WMR with M2. For instance, suppose the control input γ_2 of a WMR with M3 is chosen as $\gamma_2 = -\delta_2$ and the maximum magnitude of the control input is lower than the maximum magnitude of the perturbation $\delta_2(t)$ for some time interval, i.e., $|\gamma_2| < \sup_{t\geq 0}|\delta_2(t)|$. Then, the point system $\dot{\xi}$ of a WMR with M3 becomes

$$\dot{\xi} = \begin{bmatrix}v\cos(\theta + \gamma_2 + \delta_2)\\ v\sin(\theta + \gamma_2 + \delta_2)\end{bmatrix} \tag{74}$$

with a nonzero $\gamma_2 + \delta_2$. Similarly, by geometric relation (1), the point subsystem of a WMR with M2 (47) can be expressed in the form of

$$\dot{\xi} = \begin{bmatrix} v\cos(\theta+\delta_2) \\ v\sin(\theta+\delta_2) \end{bmatrix}. \tag{75}$$

We can see that (74) has the same form as (75). Hence, a WMR with M3 has the same point subsystem of a WMR with M2 under condition $|\gamma_2| < \sup_{t\geq 0}|\delta_2(t)|$. This shows that a WMR with M3 possesses an unmatched kinematic perturbation if the secondary control γ_2 cannot completely eliminate δ_2 due to the control input's maximum limit. Nevertheless, it is clear that a WMR with M3 in general has a better controllability than a WMR with M2. In the sequel, we highlight the implications of these results on the WMR tracking and path following problems.

V. WMR Tracking Problem

In this section, we study the tracking and path-following control problem under the influence of the kinematic perturbations due to skidding and slipping. Path following is a special case of tracking control problem in the sense that the path following problem only considers lateral and orientation errors; whereas the tracking control problem encompasses lateral, longitudinal, and orientation errors. In this section, we focus on the tracking problem.

A tracking control problem is to maneuver the WMR to follow a virtual WMR. In this paper, we consider the *posture tracking error* [31]

$$\tilde{q} = \begin{bmatrix} \tilde{\xi} \\ \tilde{\theta} \end{bmatrix} = \begin{bmatrix} \cos(\theta) & \sin(\theta) & 0 \\ -\sin(\theta) & \cos(\theta) & 0 \\ 0 & 0 & 1 \end{bmatrix} \begin{bmatrix} x_r - x \\ y_r - y \\ \theta_r - \theta \end{bmatrix}. \tag{76}$$

The reference trajectory (x_r, y_r, θ_r) represents the point coordinates and orientation of a reference virtual WMR that satisfies

$$\begin{bmatrix} \dot{x}_r \\ \dot{y}_r \\ \dot{\theta}_r \end{bmatrix} = \begin{bmatrix} v_r\cos(\theta_r) \\ v_r\sin(\theta_r) \\ \omega_r \end{bmatrix}. \tag{77}$$

$\tilde{\xi}$ denotes the point tracking error and $\tilde{\theta}$represents the orientation error. It can be shown that the dynamics of $\tilde{q}$ can be described by

$$\dot{\tilde{\xi}} = f^3_{m+s} \tag{78}$$

$$\dot{\tilde{\theta}} = \omega_r - f^2_{m,s} \tag{79}$$

where

$$f^3_2 = \begin{bmatrix} v_r\cos\theta - v_l + \tilde{y}\omega \\ -\tilde{x}\omega + v_r\sin\tilde{\theta} - v_y \end{bmatrix} \tag{80}$$

$$f^3_3 = \begin{bmatrix} v_r\cos\theta - v_l\cos\gamma_2 + \tilde{y}\omega \\ -\tilde{x}\omega + v_r\sin\tilde{\theta} - v\sin(\gamma_2+\delta_2). \end{bmatrix} \tag{81}$$

One assumption that is usually imposed on the moving reference trajectory in the tracking control problem is stated next.

Assumption 2: The yaw rate ω_r, velocity v_r, and its derivative ($\dot{q}_r$) of a reference trajectory are bounded, furthermore

$$\lim_{t\to\infty} v_r \neq 0. \tag{82}$$

WMR *point tracking problem* in the presence of skidding and slipping is said to be solvable if for a small initial tracking error $\tilde{q}(0)$, there exists a control input $\mathbf{U}(t)$ such that the point error $\tilde{\xi}$ converges to zero; and the WMR *posture tracking problem* in the presence of skidding and slipping is said to be solvable if for a small initial tracking error $\tilde{q}(0)$, there exists a control input $\mathbf{U}(t)$ such that $\tilde{q}$ converges to zero. Many controllers were proposed to solve the posture tracking problem for the Type (2,0) configuration [4], [5], [30], [32] under the nonskidding and nonslipping assumptions. We will show that there exists a control input such that a WMR with M2 in the presence of skidding and slipping is able to track the virtual WMR with the point tracking error converging to zero. Additionally, we show that there exists a control law such that the posture tracking error of a WMR with M3 in the presence of skidding and slipping converges to zero. The following result summarizes this finding.

Theorem 3: Assume that the perturbations $\{\delta_1, \delta_2, d\}$ satisfy Assumption 1. Then, in the presence of skidding and slipping,

1) a WMR with M2, described by (78), is point tracking solvable, but not posture tracking solvable.
2) a WMR with M3, described by (78) and (79), is posture tracking solvable.

Proof: Consider a WMR with M2 for the nominal case (in the absence of skidding and slipping), where the tracking error dynamics $\dot{\tilde{q}}$ is as follows:

$$\dot{\tilde{x}} = v_r\cos\tilde{\theta} - v_l + \omega\tilde{y} \tag{83}$$

$$\dot{\tilde{y}} = v_r\sin\tilde{\theta} - \omega\tilde{x} \tag{84}$$

$$\dot{\tilde{\theta}} = \omega_r - \omega. \tag{85}$$

Integrator backstepping methodology [33] has been applied for the WMR tracking control problem in the absence of wheel skidding and slipping. The reader may refer to [4] and [5] for further details. Here, we show that integrator backstepping can also be applied to solve the point tracking problem in the presence of skidding and slipping.

In the absence of skidding and slipping effects, it has been shown in [4] that by choosing $\tilde{\theta}$ as a virtual control input for point error subsystem (83) and (84), there exists a velocity control $v_l = \alpha_1$, a continuously differentiable feedback control law

$$\tilde{\theta} = \alpha_2(\tilde{\xi}) \tag{86}$$

and a positive definite function $V_1(\tilde{\xi})$ such that its derivative satisfies

$$\dot{V}_1 \leq -W(\tilde{\xi}) \leq 0 \tag{87}$$

where $W(\xi)$ is a positive definite function. Let $z = \tilde{\theta} - \alpha_2$. Then, by integrator backstepping, there exists a positive-definite function

$$V_2(\tilde{\xi}, z) = V_1 + \frac{1}{2}z^2 \tag{88}$$

and a feedback control law ω that renders $(\tilde{\xi}, z) \to 0$ as $t \to \infty$.

In the skidding and slipping case, we show the following invertible auxiliary inputs

$$v_l = r\dot{\varphi} - d \tag{89}$$

$$\omega = f_{m,s}^2 \tag{90}$$

can eliminate the input-additive and matched perturbations inherent in the kinematic model of a WMR with M2. As a result, the tracking error dynamics of a WMR with M2 can be expressed as

$$\dot{\tilde{x}} = v_r \cos\tilde{\theta} - v_l + \omega\tilde{y} \tag{91}$$

$$\dot{\tilde{y}} = v_r \sin\tilde{\theta} - \omega\tilde{x} - v_y \tag{92}$$

$$\dot{\tilde{\theta}} = \omega_r - \omega \tag{93}$$

where v_l and ω are the transformed control inputs that can be converted to original control input $(r\dot{\varphi}, \gamma_1)$. Note that in the case of skidding and slipping, an additional unmatched term v_y appears in the lateral error dynamic $\dot{\tilde{y}}$ that suggests the choice of $v_l = \alpha_1$ and a differentiable feedback control law

$$\begin{aligned}\tilde{\theta} &= \sin^{-1}\{\sin\alpha_2 + \frac{v_y}{v_r}\}\\ &= \alpha_3\end{aligned} \tag{94}$$

rendering the derivative of $\dot{V}_1$ to satisfy condition (87). Similarly, by defining $z = \tilde{\theta} - \alpha_3$, we show that there exists a positive-definite function

$$V_2(\tilde{\xi}, z) = V_1 + \frac{1}{2}z^2 \tag{95}$$

and a control law ω such that $(\tilde{\xi}, z) \to 0$ as $t \to \infty$ based on integrator backstepping.

On the other hand, it is easy to show that the WMR is not posture tracking solvable. Since Theorem 1 indicates that a WMR with M2 cannot control its position without compromising the WMR's orientation θ if δ_2 in nonzero, we conclude that the orientation of the WMR cannot approach θ_r when the WMR's reference point converges to the desired reference point trajectory (x_r, y_r).

As for the WMRs with M3, the proof is straightforward after applying Lemma 2. Since the WMR is input equivalent to a nominal Type (2,0) WMR, there exist many tracking controllers that were designed based on nonskidding and nonslipping assumptions [4], [30], [32]; therefore, a WMR with M3 is posture tracking solvable and this completes the proof.

Remark 7: Theorem 3 implies that there exists a control input that drives a WMR with M2 such that the point error converges to zero if the unmatched perturbation v_y satisfies equality (94). In addition, these results also indicate the WMR's orientation has to be "compromised" to achieve zero-point tracking error if the skidding perturbation δ_2 is nonzero. Achieving good point tracking performance is desirable, and in many practical cases, is sufficient. In some strict cases, the orientation error is as important as the point tracking error. The following results provide a measure on the orientation error while the point tracking error converges to zero.

Theorem 4: Suppose that there exists a continuously differentiable control input $\mathbf{U}(t)$ such that the point tracking error $\tilde{\xi}$ converges to zero. Then

1) the steady-state orientation error $\tilde{\theta}$ of a WMR with M2 is

$$\lim_{t\to\infty}\left(\tilde{\theta}(t) - \delta_2(t)\right) = 0 \tag{96}$$

2) the steady-state orientation error $\tilde{\theta}$ of a WMR with M3 is

$$\lim_{t\to\infty}\left(\tilde{\theta}(t) - \gamma_2(t) - \delta_2(t)\right) = 0. \tag{97}$$

Proof: We first consider the case of a WMR with M2. By assumption, the point tracking error $\tilde{\xi}$ is bounded and approaches zero. Suppose that $v_r, \dot{v}_r, \omega_r, \dot{\omega}_r$ of the reference trajectory are bounded, the boundedness of $\tilde{\xi}$ and differentiability of the control input $\mathbf{U}$ guarantee the boundedness of $\ddot{\tilde{\xi}}$; hence, $\dot{\tilde{\xi}}$ is uniformly continuous. By assumption, $\tilde{\xi}$ converges to zero. Therefore, by Barbalat lemma [34], we conclude that $\dot{\tilde{\xi}} \to 0$ as $t \to \infty$. One essential observation is that for any well-defined control input, the error dynamics of $\tilde{y}$ is governed by

$$\dot{\tilde{y}} = -\tilde{x}\omega + v_r \sin\tilde{\theta} - v_y \tag{98}$$

and $(\tilde{\xi}, \dot{\tilde{\xi}}) \to 0$ as $t \to \infty$ implies

$$\lim_{t\to\infty}\left(\sin\tilde{\theta} - \frac{v_y}{v_r}\right) = 0. \tag{99}$$

Since $\dot{\tilde{\xi}} \to 0$ means $v \to v_r$ as $t \to \infty$, geometric relation (1) leads (99) to

$$\lim_{t\to\infty}\left(\tilde{\theta}(t) - \delta_2(t)\right) = 0. \tag{100}$$

We can also show that $(\tilde{\xi}, \dot{\tilde{\xi}}) \to 0$ as $t \to \infty$ for a robot with M3. The error dynamic equation $\dot{\tilde{y}} = -\tilde{x}\omega + v_r \sin\tilde{\theta} - v\sin(\gamma_2 + \delta_2)$ of an M3 robot implies

$$\lim_{t\to\infty}\left(\sin\tilde{\theta} - \frac{v\sin(\gamma_2 + \delta_2)}{v_r}\right) = 0. \tag{101}$$

Similarly, $v \to v_r$ as $t \to \infty$. Hence, (101) leads to (97), and this completes the proof.

Theorem 4 indicates the steady-state orientation error of a WMR with M2 as the slip angle δ_2. On the other hand, a WMR with M3 does not have this limitation if the steerable wheel γ_2 is properly designed to compensate against perturbation δ_2.

Remark 8: Equality (97) suggests that the steady-state orientation error can be completely eliminated if the steering angle γ_2 of a maneuverability three WMR is properly chosen such that the steady-state orientation error approaches zero. These findings show that it is impossible for a WMR with M2 to solve the posture tracking problem if the slip angle δ_2 is nonzero. On the other hand, there exists a control input $\mathbf{U}(t)$ such that the posture tracking error of a WMR with M3 converges to zero.

Remark 9: One final point to note is that although the results are developed from kinematic perspectives, they provide many useful practical applications. For example, consider a port, where there are many large automatic guidance vehicles. Although the vehicles are travelling at low speed, the tires of these vehicles suffer from tire deformation due to heavy loads that they are carrying. Hence, high-precision kinematic controllers can be developed based on the kinematic models and the controllability insights gained in this paper.

VI. Concluding Remark

The purpose of this paper is to develop a set of kinematic models for four generic WMRs to study the behavior of the WMRs in the presence of wheel skidding and slipping from a control perspective. By using explicit descriptions to describe the kinematic perturbations induced by wheel skidding and slipping, the kinematic models lead us to the formulation of disturbance perturbations and associated properties. The formulations and developed models are unified for the four configurations of WMRs. The disturbance perturbations are classified in the perspective of control designs. In particular, we have various types of the perturbations and we offer some comparison as follows.

Among these perturbations, input-related (input-additive, input-multiplicative) and matched perturbations reduce the effectiveness of control inputs. But these types of perturbations can be easily compensated if the measurements of these uncertainties become available. On the other hand, an unmatched perturbation cannot be compensated by control input directly. The existence of the unmatched perturbation in lower maneuverability WMRs suggests that a robust control approach is not advisable. In contrast, even though there is no unmatched perturbation for the case of a WMR with M3, the nonaffine input structure of these WMRs suggests that a robust control approach is also not recommended.

Despite the difficulties resulting from the unmatched perturbation of a WMR with M2, Theorem 3 shows that the unmatched perturbation can still be compensated using the WMR's orientation to control the WMR's reference point if the measurement of the unmatched perturbation is available. This result suggests that a *backstepping* control methodology is useful to design a controller to achieve point tracking maneuver if the information of the kinematics perturbations due to wheel skidding and slipping are available. Besides the possible control strategy that has been gained from these results, we also provide a measure on the orientation error for the WMR to achieve this point tracking maneuver.

From this development, we show that a WMR with higher maneuverability is more controllable than a WMR with lower maneuverability. These results have important implications on formulating control objectives for each class of WMRs. Finally, the explicit descriptions of the kinematic perturbations sheds some light and motivation on the types of navigation sensors suitable for this application. Currently, we are researching on the perturbation estimation and control design problems based on the development of this paper. Several results with real-time implementations of control laws have been developed.

Appendix

The following results are obtained from [29]. Readers are referred to the article for details.

Consider a nonlinear systems in the form

$$\dot{x} = f(x) + \sum_{i=1}^{m} g_i(x) u_i x \in R^n, \quad u \in R^m. \tag{102}$$

The *accessibility algebra* $\mathcal{C}$ of the control system (102) is the smallest subalgebra of $\mathcal{V}(R^n)$ that contains $f, g_1, \ldots, g_m$. Note that all the repeated Lie brackets of these vector fields also belong to $\mathcal{C}$. The accessibility distribution $\triangle_{\mathcal{C}}$ of system (102) is defined as

$$\triangle_{\mathcal{C}} = \operatorname{span}\{v | v \in \mathcal{C}\}. \tag{103}$$

The following sufficient condition utilizes accessibility distribution for controllability test that is stated as follows.

Theorem 5: If the accessibility rank condition

$$\dim \triangle_{\mathcal{C}}(x_0) = n \tag{104}$$

holds, then the control system (102) is locally accessible from x_0. If the accessibility rank condition holds for all $x \in R^n$, the system is locally accessible. Conversely, if system (102) is locally accessible, then $\dim \triangle_{\mathcal{C}} = n$ holds in an open and dense subset of R^n.

Moreover, if Theorem (5) is applied to a driftless control system

$$\dot{x} = \sum_{i=1}^{m} g_i(x) u_i x \in R^n, \quad u \in R^m \tag{105}$$

it provides a sufficient condition for controllability.

References

[1] G. Campion, G. Bastin, and B. d'Andréa Novel, "Structural properties and classification of kinematic and dynamic models of wheeled mobile robots," in *Proc. 1993 IEEE Int. Conf. Robot. Autom.*, Atlanta, GA, May, vol. 1, pp. 462–469.

[2] G. Campion, G. Bastin, and B. d'Andréa Novel, "Structural properties and classification of kinematic and dynamic models of wheeled mobile robots," *IEEE Trans. Robot. Autom.*, vol. 12, no. 1, pp. 47–61, Feb. 1996.

[3] Y. F. Zheng, *Recent Trends in Mobile Robots*. Singapore: World Scientific, 1993.

[4] Z. P. Jiang and H. Nijmeijer, "Tracking control of mobile robots: A case study in backstepping," *Automatica*, vol. 33, no. 7, pp. 1393–1399, 1997.

[5] Z. P. Jiang and H. Nijmeijer, "A recursive technique for tracking control of nonholonomic systems in chained form," *IEEE Trans. Autom. Control*, vol. 44, no. 2, pp. 265–279, Feb. 1999.

[6] D. Wang and G. Xu, "Full-state tracking and internal dynamics of nonholonomic wheeled mobile robot," *IEEE Trans. Mechatronics*, vol. 8, no. 2, pp. 203–214, Jun. 2003.

[7] B. d'Andréa Novel, G. Campion, and G. Bastin, "Control of wheeled mobile robots not satisfying ideal velocity constraints: A singular perturbation approach," *Int. J. Robust Nonlinear Control*, vol. 5, pp. 243–267, 1995.

[8] W. E. Dixon, D. M. Dawson, and E. Zergeroglu, "Nonlinear control of wheeled mobile robot," in *Lecture Notes in Control and Information Sciences*. New York: Springer-Verlag, 2000.

[9] B. Thuilot, C. Cariou, and P. Martinet, "Automatic guidance of a farm tractor along curved paths, using CP-DGPS," in *Proc. 2000 IEEE Int. Conf. Robot. Autom.*, pp. 674–679.

[10] C. Samson, "Path following and time-varying stabilization of wheeled mobile robot," in *Proc. 2nd Int. Conf. Autom., Robot. Comput. Vis.*, Singapore, 1992, pp. RO-13.1.1–RO-13.1.5.

[11] C. Samson, "Control of chained systems: Application to path following and time-varying point stabilization of mobile robots," *IEEE Trans. Autom. Control*, vol. 40, no. 1, pp. 64–70, Jan. 1995.

[12] A. M. Bloch, M. Reyhanoglu, and N. H. McClamroch, "Control and stabilization of nonholonomic dynamic systems," *IEEE Trans. Autom. Control*, vol. 37, no. 11, pp. 1746–1757, Oct. 1992.
[13] A. Astolfi, "Discontinuous control of nonholonomic systems," *Syst. Control Lett.*, vol. 27, pp. 37–45, 1996.
[14] C. Samson, "Velocity and torque feedback control of a nonholonomic cart," in *Advanced Robot Control* (Lecture Notes in Control and Information Science 162), C. Canudas de Wit, Ed. Berlin, Germany: Springer-Verlag, 1991, pp. 125–151.
[15] C. Canudas de Wit and O. J. Sørdalen, "Exponential stabilization of mobile robots with nonholonomic constraints," *IEEE Trans. Autom. Control*, vol. 37, no. 11, pp. 1791–1797, Nov. 1992.
[16] R. Fierro and F. Lewis, "Control of a nonholonomic mobile robot: Backstepping kinematics into dynamics," *J. Robot. Syst.*, vol. 14, no. 3, pp. 149–163, 1997.
[17] C. C. de Wit and H. Khennouf, "Quasi-continuous stabilizing controllers for nonholonomic systems: Design and robustness considerations," in *Proc. 3rd Eur. Control Conf.*, Rome, Italy, Sep.1995, pp. 2630–2635.
[18] M. L. Corradini, T. Leo, and G. Orlando, "Robust stabilization of a mobile robot violating the nonholonomic constraint via quasi-sliding modes," in *Proc. 1999 IEEE Int. Amer. Control Conf.*, Amsterdam, The Netherlands, vol. 6, pp. 3935–3939.
[19] M. L. Corradini, T. Leo, and G. Orlando, "Experimental testing of a discrete-time sliding mode controller for trajectory tracking of a wheeled mobile robot in the presence of skidding effects," *Int. J. Robot. Syst.*, vol. 19, pp. 177–188, 2002.
[20] W. E. Dixon, D. M. Dawson, and E. Zergeroglu, "Robust control of a mobile robot system with kinematic disturbances," in *Proc. 2000 IEEE Int. Conf. Control Appl.*, pp. 437–442.
[21] W. Leroquais and B. d' A. Novel, "Modeling and control of wheeled mobile robots not satisfying ideal velocity constraints: The unicycle case," in *Proc. 35th IEEE Conf. Decis. Control*, Dec. 1996, vol. 2, pp. 1437–1442.
[22] I. Motte and G. Campion, "A slow manifold approach for the control of mobile robots not satisfying the kinematic constraints," *IEEE Trans. Robot. Autom.*, vol. 16, no. 6, pp. 875–880, Dec. 2000.
[23] B. d'Andréa Novel, G. Campion, and G. Bastin, "Control of nonholonomic wheeled mobile robots by state feedback linearization," *Int. J. Robot. Res.*, vol. 14, pp. 543–559, Dec. 1995.
[24] D. Wang and C. B. Low, "Modeling skidding and slipping in wheeled mobile robots: Control design perspective," in *Proc. 2006 IEEE/RSJ Int. Conf. Intell. Robots Syst.*, Beijing, China, Oct., pp. 1867–1872.
[25] J. Y. Wong, *Theory of Ground Vehicles*, 3rd ed ed. New York: Wiley, 2001.
[26] C. B. Low and D. Wang, "Integrated estimation for wheeled mobile robot posture, velocities and wheel skidding & slipping perturbations," in *Proc. IEEE/ICRA Int. Conf. Robot. Autom.*, Rome, Italy, Apr. 2007, pp. 2355–2360.
[27] C. B. Low and D. Wang, "GPS-based path following control for a car-like wheeled mobile robot with skidding and slipping," *IEEE Trans. Control Syst. Technol.*, vol. 16, no. 1, pp. 340–347, Mar. 2008.
[28] C. B. Low and D. Wang, "GPS-based tracking control for a car-like wheeled mobile robot with skidding and slipping," *IEEE/ASME Trans. Mechatronics*, to be published, 2008.
[29] A. D. Luca and G. Oriolo, "Modeling and control of nonholonomic mechanical system," in *Kinematics and Dynamics of Multi-Body System, J. Angeles and A. Kecskemethy,* Eds. New York: Springer-Verlag, 1995, pp. 278–342.
[30] Y. Kanayama, "Two dimensional wheeled vehicle kinematics," in *Proc. 1994 Int. Conf. Robot. Autom.*, vol. 4, pp. 3079–3084.
[31] Y. Kanayamaa, Y. Kimura, F. Miyazaki, and T. Noguchi, "A stable tracking control method for an autonomous mobile robot," in *Proc. 1990 Int. Conf. Robot. Autom.*, pp. 384–389.
[32] W. E. Dixon, D. M. Dawson, E. Zergeroglu, and A. Behal, *Nonlinear Control of Wheeled Mobile Robots*. New York: Springer-Verlag, 1996.
[33] M. Krstic, I. Kanellakopoulos, and P. Kokotovic, *Nonlinear and Adaptive Control Design*. New York: Wiley, 1995.
[34] H. K. Khalil, *Nonlinear Systems*, 3rd ed. Englewood Cliffs, NJ: Prentice-Hall, 2001.

Danwei Wang (S'88–M'89–SM'04) received the B.E. degree in electrical engineering from the South China University of Technology, Guangzhou, China, in 1982, and the M.S.E. and Ph.D. degrees in electrical engineering from the University of Michigan, Ann Arbor, in 1984 and 1989, respectively.

Since 1989, he has been with the School of Electrical and Electronic Engineering, Nanyang Technological University, Singapore, where he is currently a Professor and the Head of the Division of Control and Instrumentation. He is an Associate Editor for the *International Journal of Humanoid Robotics*. He is the author or coauthor of more than 200 technical articles in the areas of iterative learning control, repetitive control, robust control, and adaptive control systems, as well as manipulator/mobile robot dynamics, path planning, and control. His current research interests include robotics, control theory, and applications.

Prof. Wang has been a General Chairman, a Technical Chairman, and has held various positions in international conferences, such as the International Conference on Control, Automation, Robotics, and Vision (ICARCVs) and the International Conference on Intelligent Robots and Systems (IROS). He has also been an Associate Editor of the Conference Editorial Board, IEEE Control Systems Society from 1998 to 2005. He was a recipient of the Alexander von Humboldt Fellowship, Germany.

Chang Boon Low was born in Singapore. He received the B.Eng. and Ph.D. degrees in electrical and electronic engineering from Nanyang Technological University, Singapore, in 2002 and 2007, respectively.

From 2003 to 2006, he was a Teaching Assistant with Nanyang Technological University, where he was a Research Staff from 2006 to 2007. He is currently a Member of the Technical Staff of the DSO National Laboratories, Singapore. His current research interests include control systems, unmanned air and ground vehicles, system fault diagnosis, and multivehicle cooperative systems.